

Structural Differences between Open-Chain and Macrocyclic Triene Ligands for Palladium(0): Influence on the Stability and Catalytical Properties

Anna Dachs, Judit Masllorens, Anna Pla-Quintana, and Anna Roglans*

Department of Chemistry, Universitat de Girona, Campus de Montilivi, s/n. E-17071-Girona, Spain

Jordi Farjas

Department of Physics, Universitat de Girona, Campus de Montilivi, s/n. E-17071-Girona, Spain

Teodor Parella

Servei de RMN, Universitat Autònoma de Barcelona, Cerdanyola, E-08193-Barcelona, Spain

Received June 11, 2008

Two palladium complexes containing triene-coordinated ligands, **3** and **4**, open-chain analogues of the macrocyclic palladium(0) complexes of type **1**, have been synthesized. A comparative study of both open-chain and macrocyclic complexes has been carried out, based on a NMR and X-ray structural analysis, a DSC thermal behavior assessment, and a catalytical activity evaluation in the arenediazonium and organotrifluoroborate cross-coupling Suzuki–Miyaura reaction. The 1,6,11-triene sequence has been revealed to be crucial in the great stability of this family of palladium(0) complexes.

Introduction

Palladium(0) olefin complexes have been well characterized¹ but rarely used given the predominant use of phosphane and carbene ligands for palladium as catalysts.² However, one of the most frequently used palladium(0) sources is the binuclear complex Pd₂(dba)₃ (dba = dibenzylideneacetone), which is stable to air and commercially available. The displacement of the dba by a variety of ligands including phosphanes is at the origin of its extensive use as Pd(0) precursor.^{2b,3}

Several years ago, some of us discovered a palladium(0) complex of a 15-membered triolefinic macrocycle, **1** (Figure 1),⁴ and the directed synthesis of both the ligand⁵ and the

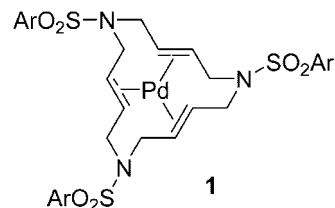


Figure 1. Palladium(0) complex of the 15-membered triolefinic macrocycle.

complex⁶ has been efficiently accomplished for a wide array of aryl groups. Interest in these compounds has now moved to their use as recoverable catalysts in various C–C bond formation reactions such as the Suzuki–Miyaura reaction,^{5a,7} telomerization of butadiene,⁸ hydroarylation of alkynes,⁹ and the Mizoroki–Heck reaction,¹⁰ as well as their applications in material sciences (crystal liquid formation¹¹ and noble metal preconcentration¹²).

* To whom correspondence should be addressed. E-mail: anna.roglans@udg.edu.

(1) (a) Choueiry, D. In *Handbook of Organopalladium Chemistry for Organic Synthesis*; Negishi, E., Ed.; Wiley: New York, 2002; Vol. 1, pp 147–187. (b) Ugo, R. *Coord. Chem. Rev.* **1968**, *3*, 319–344. (c) Davies, J. A. In *Comprehensive Organometallic Chemistry II*; Abel, E. W., Stone, F. G. A., Wilkinson, G., Eds.; Pergamon: Oxford, 1995; pp 291–390. (d) Maitlis, P. M.; Espinet, P.; Russell, M. J. H. In *Comprehensive Organometallic Chemistry I*; Abel, E. W., Stone, F. G. A., Wilkinson, G., Eds.; Pergamon: Oxford, 1982; pp 351–382 and 455–469. (e) Defieber, C.; Grützmacher, H.; Carreira, E. M. *Angew. Chem., Int. Ed.* **2008**, *47*, 4482–4502.

(2) (a) *Metal-Catalyzed Cross-Coupling Reactions*; de Meijere, A., Diederich, F., Ed.; Wiley-VCH: Weinheim, 2004. (b) *Handbook of Organopalladium Chemistry for Organic Synthesis*; Negishi, E., Ed.; Wiley: New York, 2002.

(3) (a) Takahashi, Y.; Ito, T.; Sakai, S.; Ishii, Y. *J. Chem. Soc., Chem. Commun.* **1970**, 1065–1066. (b) Mazza, M. C.; Pierpont, C. G. *Inorg. Chem.* **1973**, *12*, 2955–2959. (c) Pierpont, C. G.; Mazza, M. C. *Inorg. Chem.* **1974**, *13*, 1891–1895. (d) Ukai, T.; Kawazura, H.; Ishii, Y.; Bonnet, J. J.; Ibers, J. A. *J. Organomet. Chem.* **1974**, *65*, 253–266.

(4) Cerezo, S.; Cortès, J.; López-Romero, J.-M.; Moreno-Mañas, M.; Parella, T.; Pleixats, R.; Roglans, A. *Tetrahedron* **1998**, *54*, 14885–14904.

(5) (a) Cortès, J.; Moreno-Mañas, M.; Pleixats, R. *Eur. J. Org. Chem.* **2000**, 239–243. (b) Cerezo, S.; Cortès, J.; Galvan, D.; Lago, E.; Marchi, C.; Molins, E.; Moreno-Mañas, M.; Pleixats, R.; Torrejón, J.; Vallribera, A. *Eur. J. Org. Chem.* **2001**, 329–337.

(6) Cerezo, S.; Cortès, J.; Lago, E.; Molins, E.; Moreno-Mañas, M.; Parella, T.; Pleixats, R.; Torrejón, J.; Vallribera, A. *Eur. J. Inorg. Chem.* **2001**, 1999–2006.

(7) (a) Llobet, A.; Masllorens, E.; Moreno-Mañas, M.; Pla-Quintana, A.; Rodríguez, M.; Roglans, A. *Tetrahedron Lett.* **2002**, *43*, 1425–1428. (b) Llobet, A.; Masllorens, E.; Rodríguez, M.; Roglans, A.; Benet-Buchholz, J. *Eur. J. Inorg. Chem.* **2004**, 1601–1610. (c) Blanco, B.; Mehdi, A.; Moreno-Mañas, M.; Pleixats, R.; Reyé, C. *Tetrahedron Lett.* **2004**, *45*, 8789–8791. (d) Blanco, B.; Brissart, M.; Moreno-Mañas, M.; Pleixats, R.; Mehdi, A.; Reyé, C.; Bouquillon, S.; Hémin, F.; Muzart, J. *Appl. Catal. A: Gen.* **2006**, *297*, 117–124. (e) Moreno-Mañas, M.; Pleixats, R.; Serra-Muns, A. *Synlett* **2006**, 3001–3004. (f) Masllorens, J.; González, I.; Roglans, A. *Eur. J. Org. Chem.* **2007**, 158–166. (g) Blanco, B.; Moreno-Mañas, M.; Pleixats, R.; Mehdi, A.; Reyé, C. *J. Mol. Catal. A: Chem.* **2007**, *269*, 204–213.

(8) (a) Estrine, B.; Blanco, B.; Bouquillon, S.; Hémin, F.; Moreno-Mañas, M.; Muzart, J.; Pena, C.; Pleixats, R. *Tetrahedron Lett.* **2001**, *42*, 7055–7057. (b) Moreno-Mañas, M.; Pleixats, R.; Spengler, J.; Chevrin, C.; Estrine, B.; Bouquillon, S.; Hémin, F.; Muzart, J.; Pla-Quintana, A.; Roglans, A. *Eur. J. Org. Chem.* **2003**, 274–283.

(9) Cacchi, S.; Fabrizi, G.; Goggiani, A.; Moreno-Mañas, M.; Vallribera, A. *Tetrahedron Lett.* **2002**, *43*, 5537–5540.

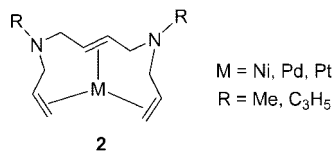


Figure 2. Pörschke's tris-ene complexes.

One aspect that has attracted our attention throughout the study is the characteristic structural features of complexes **1**, which confer an intrinsic chirality and high stability. The complexation of the metal on one of the two stereotopic faces of each of the olefins present in the structure may form various isomers, of which only the energetically favorable ones are experimentally observed by means of both NMR and X-ray techniques.¹³ The conformation of the six-membered chelate rings determines the stability of the compound and, hence, its formation. In fact, the isomers observed are the ones showing two of the cyclohexane rings in the *chair* conformation and the third in the *twist* conformation. This leads to extremely rigid and stable structures, which are more stable than other palladium(0) complexes stabilized only by olefin ligands synthesized to date.

However, it is not clear how complex **1** attains such stability. A likely answer has been outlined by Pörschke et al. when studying a series of tris-ene trigonal-planar nickel(0), palladium(0), and platinum(0) complexes (Figure 2).¹⁴ It emerged from this¹⁴ and earlier¹⁵ studies that chelating 1,6-diene ligands, and polyenes with a repetitive 1,6-diene sequence, seem to be particularly suitable for trigonal-planar coordination of group 10 metals and, at the very least, to be more suitable than 1,5-diene sequences.

This effect is striking if we compare the 1,5- and 1,6-sequences in macrocyclic complexes. Neither (*trans,trans,trans*-cyclododecatriene)palladium(0) nor (*cis,cis,cis*-cyclododecatriene)palladium(0) have so far been accessible, whereas complex **1**, the only known triene macrocyclic palladium(0) complex, has extreme stability.

In order to investigate the stability of macrocycles **1** and evaluate the contribution of the macrocyclic effect as compared to the chelate effect,¹⁶ we present here the synthesis of complexes **3** and **4** (Figure 3), open-chain analogues of macrocyclic complex **1**. We perform a complete structural characterization of the two complexes synthesized by means of NMR spectroscopy and X-ray diffraction analysis and

compare them with their macrocycle analogue, we undertake a DSC thermal stability study (differential scanning calorimetry) of both the chelate and macrocyclic complexes, and finally we make a comparative study of the catalytic activity of the two types of systems.

Results and Discussion

Preparation of Palladium(0) Complexes. (*E,E,E*)-1,16-Bis(*tert*-butyloxycarbonyl)-1,6,11,16-tetrakis[(4-methylphenyl)sulfonyl]-1,6,11,16-tetraazahexadeca-3,8,13-trienepalladium(0), **3**, and (*E,E,E*)-1,6,11,16-tetrakis[(4-methylphenyl)sulfonyl]-1,6,11,16-tetraazahexadeca-3,8,13-trienepalladium(0), **4**, were readily prepared by ligand exchange of the respective triene ligands¹⁷ and Pd₂(dba)₃ in acetonitrile at room temperature. Both complexes **3** and **4** were isolated from the reaction mixture first by filtration through Celite to remove excess palladium black and then by column chromatography on silica gel to remove the displaced dibenzylideneacetone ligand. Macrocyclic palladium complexes **1a**^{7a} and **1b**⁶ have been previously described. The four palladium(0) complexes dissolve readily in aprotic polar solvents and are air and moisture stable, both in solid state and in solution.

Structural Study by Means of NMR and X-ray Crystallography. These are ideally suited structural techniques to characterize these palladium(0)-azaalkene complexes, as shown by the detailed structural analysis carried out on analogous 15-,^{13,18} 20-,¹⁸ 25-,¹⁸ and 30-membered¹⁷ azamacrocyclic complexes. We began to analyze the structural differences between macrocycles **1a** and **1b** and open-chain palladium complexes **3** and **4** using NMR spectroscopy.

The simple ¹H and ¹³C NMR spectra of complexes **3** and **4** confirm the presence of a high symmetry in the molecule. As has been seen for analogous macrocyclic complexes **1**,¹³ no fluxional behavior takes place, as indicated by the absence of chemical exchange cross-peaks in the NOESY spectra for a wide range of temperatures and by the well-defined chemical shifts shown for the diastereotopic methylene protons. The upfield shift of the olefinic protons proves the coordination of the palladium(0) with the three olefins of the ligand, resulting in the formation of a rigid five-ring system consisting of consecutively fused three- and six-membered rings (Table 1). The coordination of the palladium to each of the two stereotopic faces of the three double bonds generates six asymmetric carbons, but only three independent pairs of asymmetric centers must be considered given the defined *trans* stereochemistry of the double bonds. After reducing the symmetrically equivalent isomers, three pairs of enantiomers, showing respectively chair/chair, chair/twist, and twist/twist conformations of the two cyclohexane rings, should be possible. Only one six-membered substructure presenting the highly rigid chair conformation, deduced from the well-characterized axial ($\delta = 1.45\text{--}1.66$ ppm) and equatorial ($\delta = 4.34\text{--}4.67$ ppm) position of the α -nitrogen methylene protons d and f ($\Delta\delta$ about 3 ppm), is seen in the ¹H NMR spectra. Therefore, it can be stated that stereoisomers containing palladacyclohexane rings with a twist conformation are not formed, which leaves just the pair of enantiomers **A1** and **A2** with an overall chair/chair conformation (Figure 4), and presenting a C₂ axis, as experimentally observed structures. Both ¹H and ¹³C NMR data (Table 1) are fully consistent with the

(10) (a) Masllorens, J.; Moreno-Mañas, M.; Pla-Quintana, A.; Roglans, A. *Org. Lett.* **2003**, *5*, 1559–1561. (b) Serra-Muns, A.; Soler, R.; Badetti, E.; Mendoza, P.; Moreno-Mañas, M.; Pleixats, R.; Sebastián, R. M.; Vallribera, A. *New J. Chem.* **2006**, *30*, 1584–1594. (c) Badetti, E.; Caminade, A.-M.; Majoral, J.-P.; Moreno-Mañas, M.; Sebastián, R. M. *Langmuir* **2008**, *24*, 2090–2101.

(11) (a) Moreno-Mañas, M.; Reichardt, C.; Sebastián, R. M.; Barberá, J.; Serrano, J. L.; Sierra, T. *J. Mater. Chem.* **2005**, *15*, 2210–2219. (b) Soler, R.; Badetti, E.; Moreno-Mañas, M.; Vallribera, A.; Sebastián, R. M.; Vera, P.; Serrano, J. L.; Sierra, T. *Liq. Cryst.* **2007**, *34*, 234–240.

(12) (a) Masllorens, J.; Roglans, A.; Anticó, E.; Fontàs, C. *Anal. Chim. Acta* **2006**, *560*, 77–83. (b) García, L.; Torrent, A.; Anticó, E.; Fontàs, C.; Roglans, A. *React. Funct. Polym.* **2008**, *68*, 1088–1096.

(13) Pla-Quintana, A.; Roglans, A.; Julián-Ortiz, J. V.; Moreno-Mañas, M.; Parella, T.; Benet-Buchholz, J.; Solans, X. *Chem.—Eur. J.* **2005**, *11*, 2689–2697.

(14) Blum, K.; Chernyshova, E. S.; Goddard, R.; Jonas, K.; Pörschke, K.-R. *Organometallics* **2007**, *26*, 5174–5178.

(15) (a) Krause, J.; Haack, K.-J.; Cestaric, G.; Goddard, R.; Pörschke, K.-R. *J. Chem. Soc., Chem. Commun.* **1998**, 1291–1292. (b) Krause, J.; Cestaric, G.; Haack, K.-J.; Seevogel, K.; Storm, W.; Pörschke, K.-R. *J. Am. Chem. Soc.* **1999**, *121*, 9807–9823.

(16) Hancock, R. D.; Martell, A. E. *Comments Inorg. Chem.* **1988**, *6*, 237–284.

(17) Pla-Quintana, A.; Roglans, A.; Parella, T.; Benet-Buchholz, J. J. *Organomet. Chem.* **2007**, *692*, 2997–3004.

(18) Pla-Quintana, A.; Torrent, A.; Dachs, A.; Roglans, A.; Pleixats, R.; Moreno-Mañas, M.; Parella, T.; Benet-Buchholz, J. *Organometallics* **2006**, *25*, 5612–5620.

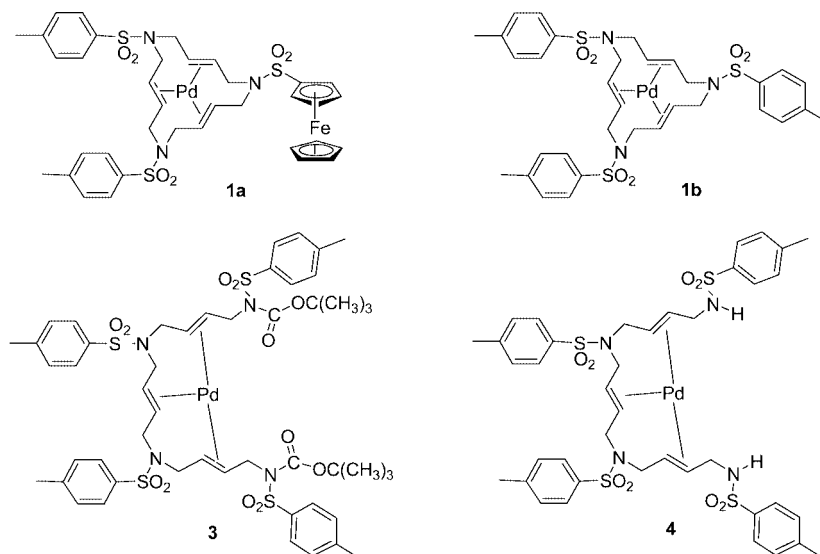


Figure 3. Palladium(0) complexes of the open-chain and macrocyclic azatriene ligands studied.

Table 1. Selected ^1H and ^{13}C NMR Chemical Shift Assignments for Palladium Complexes **3** and **4** (carbon chemical shifts shown in italics)

| compound | a | b | c | d | e | f |
|------------------|-----------------|-----------|-----------|-----------------|-----------------|-----------|
| 3 (R=Boc) | 4.94, 3.79 48.8 | 4.00 75.9 | 4.41 83.1 | 4.67, 1.58 48.6 | 4.66, 1.66 48.1 | 4.02 79.4 |
| 4 (R=H) | 3.94, 2.85 45.7 | 3.53 75.4 | 3.90 82.6 | 4.34, 1.45 48.2 | 4.54, 1.59 48.2 | 3.93 79.8 |

formation of only the pair of enantiomers **A1** and **A2** for both complexes **3** and **4**.

Due to their cyclic nature and the tight fit of the palladium, the 15-membered macrocyclic palladium(0) complexes **1** had better fixed positions in their overall structure than their open-chain analogues **3** and **4**. This is clearly indicated by the chemical shift difference in the methylene groups located α with respect to the nitrogens, as seen in our previous studies.^{13,17,18} Whereas for open-chain analogues **3** and **4** the chemical shift difference for the two methylene protons *a* (Table 1) is about 1 ppm, this difference is about 1.7 and 3.0 ppm for twist and chair conformation methylenes, respectively, in the macrocyclic complex **1**. This looseness may allow the chelate complexes to settle in a more ideal trigonal-planar coordination geometry as compared to the macrocyclic complexes. However, the actual mode of coordination is more easily studied by means of X-ray crystallography, which is the next technique we used to continue this comparative structural analysis.

Single crystals of **3** were obtained by slow diffusion of hexane into a dichloromethane/ethyl acetate solution of the complex, and the molecular structure was determined by X-ray crystallography (Table 2, Figure 5). The compound crystallizes in the monoclinic space group $P2_1/c$, with the palladium(0) atom coordinated by the three double bonds of the azatriene ligand in a trigonal planar coordination geometry. Both cyclohexanic rings have a rigid *chair* conformation (shown in Figure 6), as already deduced from the ^1H and ^{13}C NMR data, and the complex presents a C_2 symmetry axis. Both enantiomers of the favorable **A1/A2** pair are present in the crystal packing: the space group $P2_1/c$ is a centrosymmetrical space group, with the two enantiomers present in the unit cell related by an inversion center. As a result, the crystal is not chiral (racemic mixture).

As a result of the complexation, with back-donation of electron density from a filled hybrid orbital on the metal/palladium to the initially empty π^*_{2p} orbital on the olefin, an increasing hybridization of the coordinated olefinic carbon center from sp^2 to sp^3 is induced.^{1e} Consequently, the C=C bond distances are elongated, and the planarity of the sp^2 -hybridized carbon atoms is lost. These distortions are observed to a greater extent for the open-chain complex than for the macrocyclic one. For example, the olefinic C=C bond distances in **3** (1.376(4) and 1.394(6) Å) are longer than distances in **1**, containing three ferrocenyl units¹³ (1.320(3), 1.326(3), and 1.325(3) Å). On the other hand, the loss of planarity, observed by the extent to which

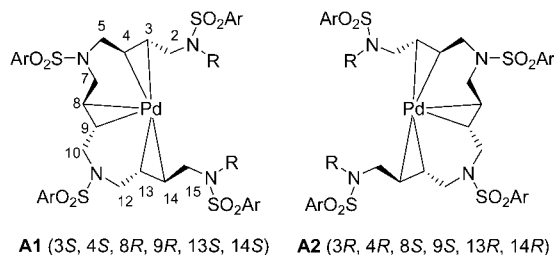


Figure 4. Pair of enantiomers **A1/A2** for palladium(0) complexes **3** (R = Boc) and **4** (R = H).

Table 2. Crystal Data for Palladium(0) Complex 3

| | |
|---|--|
| formula | C ₅₀ H ₆₄ N ₄ O ₁₂ Pd ₄ |
| fw [g · mol ⁻¹] | 1147.69 |
| crystal size [mm] | 0.3 × 0.08 × 0.08 |
| crystal color | colorless |
| temp [K] | 300(2) |
| cryst syst | monoclinic |
| space group | <i>P2/c</i> |
| <i>a</i> [Å] | 14.770(8) |
| <i>b</i> [Å] | 13.850(7) |
| <i>c</i> [Å] | 14.432(8) |
| α [deg] | 90.00 |
| β [deg] | 99.338(9) |
| γ [deg] | 90.00 |
| <i>V</i> [Å ³] | 2913(3) |
| <i>Z</i> | 2 |
| ρ [g · cm ⁻³] | 1.308 |
| absorb coeff, μ [mm ⁻¹] | 0.520 |
| θ range for data collection [deg] | 2.03 to 28.41 |
| limiting indices | -19 ≤ <i>h</i> ≤ 19, -18 ≤ <i>k</i> ≤ 18, -18 ≤ <i>l</i> ≤ 19 |
| reflns collected/unique | 41 587/7226 [<i>R</i> (int) = 0.0812] |
| completeness to θ = 28.41° [%] | 98.6 |
| absorb corr | none |
| refinement method | full-matrix least-squares on <i>F</i> ² |
| data/restraints/params | 7226/0/326 |
| goodness-of-fit (<i>F</i> ²) | 0.967 |
| final <i>R</i> indices [<i>I</i> > 2σ(<i>I</i>)] | <i>R</i> ₁ = 0.0504, <i>wR</i> ₂ = 0.1174 |
| <i>R</i> indices [all data] | <i>R</i> ₁ = 0.0940, <i>wR</i> ₂ = 0.1297 |
| largest diff peak and hole [e Å ⁻³] | 0.384 and -1.099 |

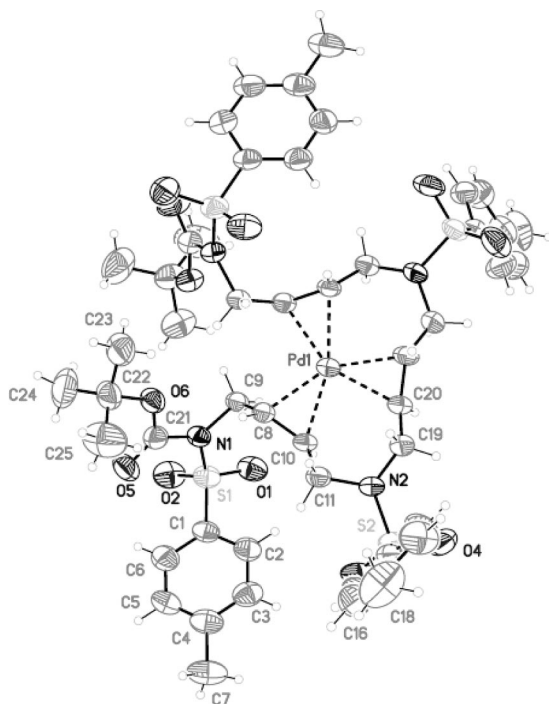


Figure 5. ORTEP plot (50%) obtained from single-crystal X-ray structure analysis of **3**. Selected bond distances (Å): C(9)–C(10) 1.376(4); C(20)–C(20′) 1.394(6); Pd(1)–C(9) 2.211(3); Pd(1)–C(10) 2.216(3); Pd(1)–C(20) 2.233(3).

the olefinic substituents are bent away from the palladium,¹⁹ is also slightly greater for palladium(0) complex **3** (on average for the three double bonds approximately 19°) than for the macrocyclic complexes **1** (17°).¹³ Furthermore, it is observed that the loss of planarity is slightly greater for the central double bond of the open-chain ligand than for those located externally,

(19) Calculated by comparison of the torsion angle of carbon centers C(19)–C(20)–C(20′)–C(19′) and C(8)–C(9)–C(10)–C(11) from the theoretical planarity for this angle in an uncomplexed olefin.

which is in agreement with the central C=C bond being longer than the external. These are indications of a more optimal back-bonding from the palladium(0) atom in the acyclic ligands.

Another effect observed upon complexation is the fixation of the orientation for the double bonds with the palladium–alkene bonds that are approximately perpendicular to the plane of the olefin. The three palladacyclopropane rings in complex **3** create a three-paddled helix centered at the metal atom. Each of these three-membered rings is rotated through the palladium–alkene bond by 10.7° (Pd–C9–C10) and 14.6° (Pd–C20–C20′) with respect to the plane defined by the palladium atom and the central point of each olefin. This rotation was about 20° for the macrocyclic complexes **1**.¹³ These differences (Δ = 9.3° and 5.4°) are schematically displayed in Figure 7. The fact that the back-bonding from the metal to the olefin is optimal when the three double bonds are located exactly on the same plane as the metal is an indication again that it is more effective for the open-chain complex **3** than for the macrocyclic analogue **1**.

To sum up, the X-ray structure shows that the back-bonding is more optimal for the open-chain complex **3** than for the macrocyclic complex **1**. This can be ascribed to the less restricted conformation of the open-chain ligand, which allows for more optimal coordination geometry.

Thermal Behavior Studies by Means of Differential Scanning Calorimetry (DSC). The next step was to analyze the differences in thermal behavior of the two types of complexes. Thermal analysis is a group of techniques in which a physical property of a substance and/or its reaction products is measured as a function of temperature while the substance is subjected to a controlled temperature program.²⁰ In particular, the DSC technique measures the heat exchange between the substance and an inert reference. Therefore, DSC is especially suited for the analysis of thermal decomposition, melting, and crystallization of substances.

The thermal behavior of complexes **3**, **4**, **1a**, and **1b**, as well as their respective free ligands **5**, **6**, **7a**, and **7b**, was studied by means of DSC under flowing N₂ (see Table 3). Crystalline samples of all compounds were subjected to two consecutive cycles of heating–cooling at a scan rate of 10 and –20 K/min, and the content of the crucible was analyzed by means of ¹H NMR after DSC analysis. In order to observe the formation of volatile compounds, the sample mass was measured before and after the DSC measurement. No mass variation was observed for complexes **3** and **4**, while a mass loss of 3.7 and 5.7% was observed for compounds **1a** and **1b**, respectively. Unlike complexes **3** and **4**, macrocyclic complexes **1a** and **1b** showed an endothermic peak at around 110 °C (112 °C for **1a** and 110 °C for **1b**). Two ¹H NMR spectra were performed: the first was on the compound before DSC analysis, and the second, on a sample of the crucible removed from the heat just after this peak. This second spectrum did not show the characteristic signal of dichloromethane at δ = 5.32 ppm.²¹ The mass loss and the endothermic peak are therefore ascribed to dichloromethane desolvation.

All four ligands **5**, **6**, **7a**, and **7b** showed an endothermic peak during the first heating ramp assigned to the melting of the compound (entries 1, 3, 5, and 7, Table 3). On the other hand, the complexes **3**, **4**, **1a**, and **1b** underwent melting superimposed

(20) L'vov, B. V. *Thermal Decomposition of Solids and Melts: New Thermochemical Approach to the Mechanism, Kinetics and Methodology*; Springer: Berlin, 2007.

(21) The dichloromethane could not be removed from the starting macrocyclic complexes **1a** and **1b** by drying it under vacuum for several days at room temperature.

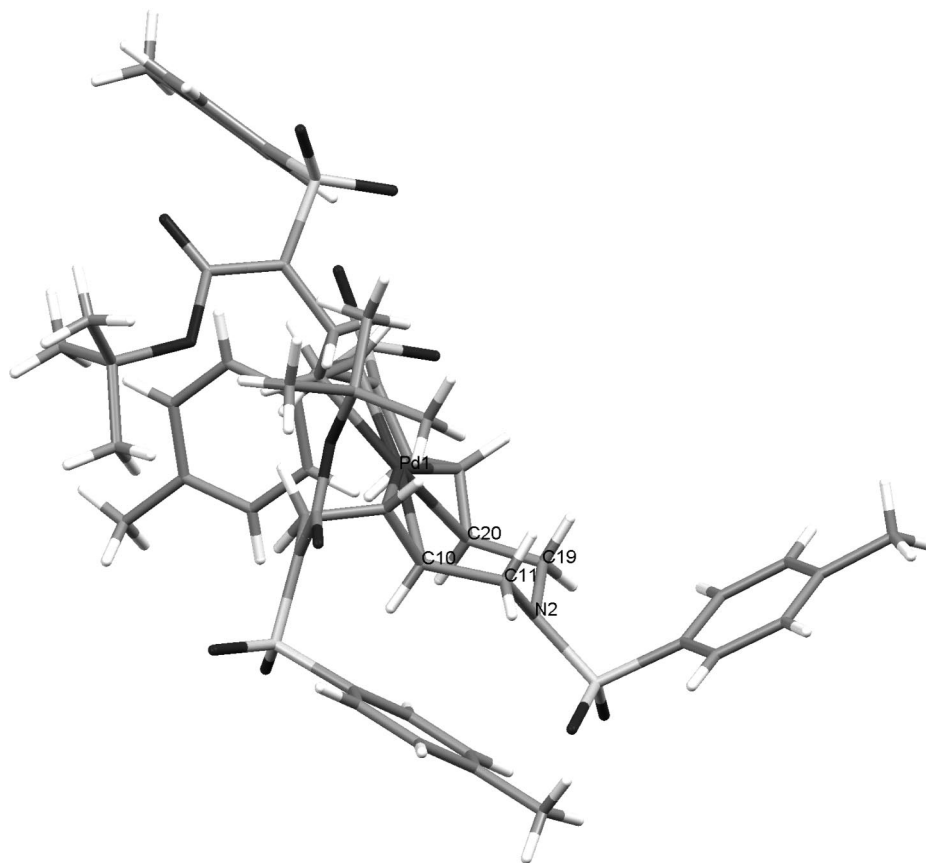


Figure 6. Representation of X-ray structure of complex **3** in which the chair conformation of palladacyclohexane ring Pd(1)–C(20)–C(19)–N(2)–C(11)–C(10) is shown.

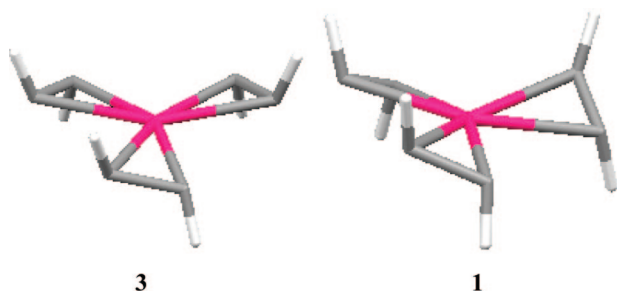


Figure 7. Simplified view (the units CH₂NCH₂ of the cyclohexane rings have been omitted for clarity) of the X-ray structure for the open-chain palladium(0) complex **3** and the macrocyclic palladium(0) complex **1** presenting three ferrocenyl units on the sulfonamide moieties.¹⁵

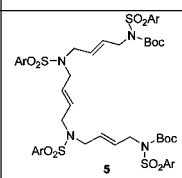
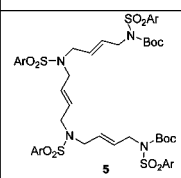
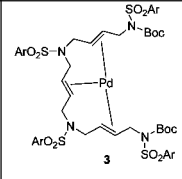
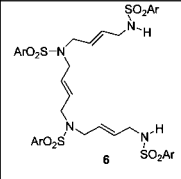
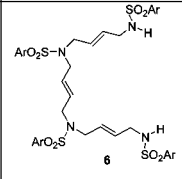
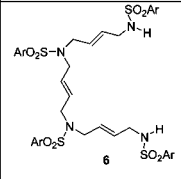
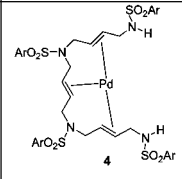
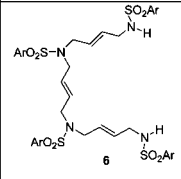
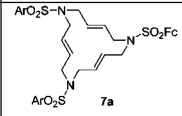
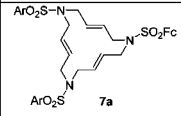
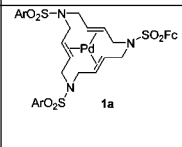
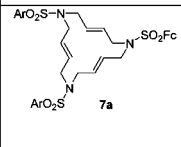
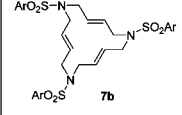
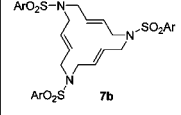
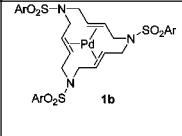
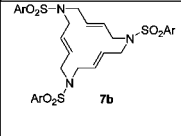
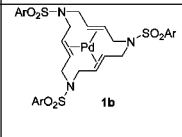
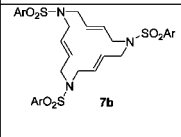
on a decooordination process (entries 2, 4, 6, and 8, Table 3). This indicates that the complex is unstable in its liquid form at the melting temperature and therefore decomposes as soon as it melts. In all cases, the decomposition observed due to the decooordination of palladium(0) from the ligand was confirmed from ¹H NMR spectra. Since melting and decomposition processes occur simultaneously, it is not possible to determine the activation energy of the decomposition process, which took place in its liquid phase, and therefore the stability of these complexes cannot be measured. However, there are two significant differences between the open-chain and macrocyclic complexes: macrocyclic complexes melt at higher temperatures (i.e., are stable at higher temperatures in their solid state) and open-chain complexes exhibit a pronounced exothermic signal related to the decooordination process. The energy evolved during decooordination of complexes **1a** and **1b** is so small that it is

hidden inside the melting peak. Thus, the energy difference between the compound and the product after decooordination is very small for compounds **1a** and **1b**, while the energy difference is significant for complexes **3** and **4** (see DSC curves in the Supporting Information). This fact might be derived from a major increase in strain energy that occurs in complex formation for the open-chain analogue as compared to the macrocyclic complex formation. Indeed, the olefins in the macrocyclic ligand are preorganized for palladium complex formation and prestrained due to its macrocyclic nature, as opposed to the open-chain ligands.¹⁶ Furthermore, complex **3** showed the more pronounced exothermic decomposition concomitant with Boc cleavage.

The absence of any peak in the cooling thermogram for all complexes confirmed the vitrification of the samples upon cooling.²² The compounds have a complex crystal structure that cannot be formed under the experimental conditions used for the present DSC analysis. However, in the second heating cycle compound **1b** first crystallizes (exothermic peak at 110 °C) and afterward melts (endothermic peak at 158 °C). This indicates that compound **1b** crystallizes more easily than the other compounds. Note that the temperature difference between the melting in the first heating cycle (178 °C, entry 8) and the second (158 °C, entry 9) indicates that the decooordination of the palladium from the ligand reduces the melting point.

Catalytical Activity of Palladium(0) Complexes. Finally we evaluated the likely differential behavior in the catalytical activity of open-chain and macrocyclic palladium(0) complexes. As already stated in the Introduction, macrocyclic palladium(0) complexes **1** have been shown to be very robust and effective recoverable catalysts in a number of C–C bond formation

Table 3. DSC Data for Open-Chain and Macrocyclic Palladium(0) Complexes and Their Corresponding Ligands^a

| Entry | Compound ^b | DSC signal / assignation | Final product ^{b,c} |
|----------------|---|--|---|
| 1 |  | Endothermic melting peak with shoulder. Onset at 102°C and peak at 131°C |  |
| 2 |  | Melting with exothermic process due to palladium decoordination and Boc cleavage. Onset at 140°C |  |
| 3 |  | Endothermic melting peak with shoulder. Onset at 148°C and peak at 164°C |  |
| 4 |  | Melting with exothermic process due to palladium decoordination. Onset at 120°C |  |
| 5 |  | Endothermic melting peak with shoulder. Onset at 154°C and peak at 191°C |  |
| 6 |  | Endothermic peak due to CH ₂ Cl ₂ ^d desolvation. Onset at 112°C and peak at 124°C. Endothermic melting with two overlapping peaks. Onset at 162°C and peaks at 179°C and 184°C |  |
| 7 |  | Endothermic melting peak. Onset at 184°C and peak at 199°C |  |
| 8 |  | Endothermic peak due to CH ₂ Cl ₂ desolvation. Onset at 110°C and peak at 136°C. Endothermic melting peak. Onset at 178°C and peak at 181°C |  |
| 9 ^e |  | Exothermic crystallization peak. Onset at 110°C, peak at 121°C Endothermic melting peak. Onset at 158°C, peak at 166°C |  |

^a All samples were submitted to two consecutive heating/cooling cycles at a scan rate of 10 and -20 K/min, respectively. The starting and stopping temperatures were adapted for each case. Upon cooling, all the samples vitrified (macroscopic observation). No signal was observed for the second heating cycle, with the exception of complex **1b**. ^bAr stands for 4-methylphenyl; Fc stands for ferrocenyl. ^cThe final products were characterized by means of ¹H NMR of the sample inside the crucible after the DSC analysis. ^dThe peak was assigned as loss of dichloromethane by running ¹H NMR on the sample before the DSC analysis and on the same sample stopped just after the assigned DSC peak. ^eDSC peaks observed during the second heating cycle of the sample analyzed in entry 8.

reactions.^{7–10} The great stability of these compounds facilitates their recovery after the reaction, but it can also constitute a drawback if it reduces the activity of the catalyst. The reaction of choice was the Suzuki–Miyaura cross-coupling of arene-diazonium salts with potassium organotrifluoroborates,²³ for

which catalyst **1a** had already been tested with excellent catalyst recovery results, but only moderate yields.^{7f}

Chelated palladium(0) complexes **3** and **4** were tested as catalysts for the mentioned Suzuki–Miyaura cross-couplings and compared with the previously obtained results for macro-

Table 4. Suzuki–Miyaura Reactions between Arenediazonium Tetrafluoroborates and Potassium Organotrifluoroborates^d

| entry | ArN ₂ BF ₄ /R ₁ | ArBF ₃ K/R ₂ | catalyst | added base | time (h) | product/yield (%) | catalyst recovery (%) ^a |
|-----------------|--|------------------------------------|-----------|--------------------------------|----------|-----------------------------|------------------------------------|
| 1 | 8a /H | 9a /H | 3 | | 24 | 10a /0 | 0 |
| 2 | 8a /H | 9a /H | 3 | K ₂ CO ₃ | 2.25 | 10a /64 | 85 |
| 3 | 8a /H | 9a /H | 4 | K ₂ CO ₃ | 22 | 10a /65 | 0 |
| 4 ^c | 8a /H | 9a /H | 1a | | 15 | 10a /63 | 100 |
| 5 | 8a /H | 9b /F | 3 | | 24 | 10b /0 ^b | 0 |
| 6 | 8a /H | 9b /F | 3 | K ₂ CO ₃ | 28 | 10b /55 | 97 |
| 7 | 8a /H | 9b /F | 4 | | 24 | 10b /0 ^b | 0 |
| 8 ^c | 8a /H | 9b /F | 1a | | 17 | 10b /54 | 100 |
| 9 | 8b / <i>p</i> -OCH ₃ | 9a /H | 3 | K ₂ CO ₃ | 16 | 10c /28 ^b | 90 |
| 10 | 8b / <i>p</i> -OCH ₃ | 9a /H | 4 | K ₂ CO ₃ | 23 | 10c /54 | 0 |
| 11 ^c | 8b / <i>p</i> -OCH ₃ | 9a /H | 1a | | 17 | 10c /63 | 100 |
| 12 | 8c / <i>m</i> -CH ₃ | 9a /H | 3 | K ₂ CO ₃ | 28 | 10d /53 | 98 |
| 13 | 8c / <i>m</i> -CH ₃ | 9a /H | 3 | CaCO ₃ | 24 | 10d /38 | 65 |
| 14 | 8c / <i>m</i> -CH ₃ | 9a /H | 4 | K ₂ CO ₃ | 24 | 10d /55 | 0 |
| 15 ^c | 8c / <i>m</i> -CH ₃ | 9a /H | 1a | | 19 | 10d /30 | 100 |
| 16 | 8d / <i>p</i> -CH ₃ | 9a /H | 3 | K ₂ CO ₃ | 24 | 10e /24 ^b | 100 |
| 17 | 8d / <i>p</i> -CH ₃ | 9a /H | 3 | CaCO ₃ | 25 | 10e /44 ^b | 31 |
| 18 | 8d / <i>p</i> -CH ₃ | 9a /H | 4 | K ₂ CO ₃ | 24 | 10e /53 | 0 |
| 19 ^c | 8d / <i>p</i> -CH ₃ | 9a /H | 1a | | 19 | 10e /39 | 100 |
| 20 | 8a /H | 9c /OCH ₃ | 3 | K ₂ CO ₃ | 24 | 10c /85 | 100 |
| 21 ^c | 8a /H | 9c /OCH ₃ | 1a | | 19 | 10c /43 | 100 |
| 22 | 8b / <i>p</i> -OCH ₃ | 9b /F | 3 | K ₂ CO ₃ | 26 | 10f /91 | 100 |
| 23 ^c | 8b / <i>p</i> -OCH ₃ | 9b /F | 1a | | 17 | 10f /42 | 100 |

^a Palladium(0) complex was recovered by column chromatography on silica gel. ^b The product from diazonium salt homocoupling was isolated from the reaction mixture. ^c Reaction published elsewhere (ref 7f). ^d Reactions were carried out under aerobic conditions with 1 equiv of **8**, 1.2 equiv of **9**, 5 mol % of the corresponding palladium(0) complex, and 1.1 equiv of base (when needed) in 1,4-dioxane at room temperature until the evolution of nitrogen gas ceased.

cyclic palladium complex **1a** using analogous reaction conditions (Table 4).

First, the same reaction conditions used for catalyst **1a**^{7f} were applied to open-chain complexes **3** and **4** (entries 1, 5, and 7 in Table 4). No cross-coupled product was obtained in any case, and we observed only either degradation of the reactants (entry 1) or the formation of the arenediazonium salt homocoupled product (entries 5 and 7). Furthermore, catalyst recovery was impossible, as it was damaged during the course of the reaction. We then decided to check the effect of adding potassium carbonate to the reaction media as a base.²⁴ The outcome of this modification depended on the catalyst used. Even though the added base enabled the reaction to a greater or lesser extent in both cases, catalyst **4**, which has its sulfonamidic nitrogens in its free form, could not be recovered presumably due to side reactions of these free nitrogens in the basic medium (entries 3, 10, 14, and 18). In the case of catalyst **3**, whose sulfonamidic nitrogens are protected by the *tert*-butyloxycarbonyl (Boc) group, the addition of potassium carbonate gave better yield and catalyst recovery than with base-free conditions (compare entry 1 with 2 and entry 5 with 6). The use of another carbonate base such as CaCO₃ always resulted in much lower catalyst recoveries (compare entry 12 with 13 and entry 16 with 17), although in one case the yield was increased (entries 16 and 17).

Once good reaction conditions were obtained for chelate palladium(0) complex **3**, the catalytic activity and catalyst recovery comparison between open-chain catalyst **3** and macrocyclic complex **1a** could be made. The behavior is not identical for all cases, but some trends can be pointed out. All the reactions took almost the same time to be completed with either the open-chain or the macrocyclic catalyst, with the

exception of the coupling of arenediazonium tetrafluoroborate **8a** and potassium phenyltrifluoroborate **9a** (entries 2 and 4). This reaction was much faster using the chelated complex **3** (2.25 h, entry 2) than macrocyclic catalyst **1a** (15 h, entry 4), achieving analogous yields and only a slight decrease in catalyst recovery (85% for **3**, 100% for **1a**). When considering the yield of the reaction, there are two cases (entries 9 and 11, entries 16 and 19) in which the yield for the open-chain catalyst **3** is decreased as compared to the macrocyclic analogue **1a**. The explanation for this decrease is the consumption of the corresponding arenediazonium salt by a homocoupling reaction. However, there are also three cases in which the yield is considerably increased when using open-chain catalyst **3** (entries 12 (53%) and 15 (30%), entries 20 (85%) and 21 (43%), entries 22 (91%) and 23 (42%)), without any significant change in the catalyst recovery or reaction time. Finally, it is found that the catalyst is always completely recovered in the case of palladium(0) macrocyclic complex **1a** and that excellent recoveries are also achieved with the open-chain analogue **3**, although these are slightly worse in two cases (entries 2 and 9).

The conclusion that can be drawn is that the activity of the open-chain analogue **3** is equal to, or in some cases even greater than, its macrocyclic counterpart **1a**. In any case, the difference is not spectacular, and hence the stability imparted by the macrocycle effect on complex **1** does not constitute a serious drawback when considering the catalytic activity, but it generally enhances the catalyst robustness and recovery.

(23) (a) Darses, S.; Jeffery, T.; Brayer, J. L.; Demoute, J. P.; Genêt, J. P. *Bull. Soc. Chim. Fr.* **1996**, 133, 1095–1102. (b) Darses, S.; Genêt, J. P.; Brayer, J. L.; Demoute, J. P. *Tetrahedron Lett.* **1997**, 38, 4393–4396. (c) Darses, S.; Michaud, G.; Genêt, J. P. *Eur. J. Org. Chem.* **1999**, 1875–1883.

(24) Bruner, H.; Le Cousturier de Courcy, N.; Genêt, J.-P. *Tetrahedron Lett.* **1999**, 40, 4815–4818.

(22) The vitrification could be macroscopically observed when opening the crucibles after DSC analysis.

Conclusions

In an attempt to find an answer to whether our 15-membered macrocyclic palladium(0) complexes **1** owe their robustness and stability mainly to the macrocyclic effect or to their 1,6,11-triene sequence, we have made a comparative study of the structural features, thermal analysis, and catalytic activity of the macrocyclic complexes **1** and their open-chain analogues **3** and **4**. Whereas the structural analysis shows that the major flexibility of the open-chain analogue allows for a more ideal planar trigonal coordination of the palladium by the three olefins present in both structures as well as a more effective back-bonding, this difference does not seem to have a major weight on the overall stabilizing effects. On the other hand, the thermal study points out a major increase of strain upon complexation of the open-chain analogues. Indeed, the olefins in the macrocyclic ligand are preorganized for palladium complex formation and prestrained due to its macrocyclic nature as opposed to the open-chain ligands. Furthermore, the catalytic activity showed by both palladium(0) complexes **1** and **3** in the Suzuki–Miyaura coupling of arenediazonium and organotrifluoroborates does not present substantial differences, which could be ascribed to a greater stability of one of the two kinds of complexes. Therefore, the great stability of both 15-membered palladium(0) complexes **1** and the open-chain analogues **3** and **4** derives mainly from the 1,6,11-triene sequence, even though the macrocyclic nature of **1** imparts more robustness to these kinds of complexes.

Experimental Section

General Procedures. Acetonitrile was degassed and dried under nitrogen by passing through solvent purification columns (MBraun, SPS-800). 1,4-Dioxane was distilled under nitrogen over sodium as the drying agent. Solvents were removed under reduced pressure with a rotary evaporator. Reaction mixtures were chromatographed on a silica gel column (230–400 mesh). Arenediazonium tetrafluoroborates **8a–d** were prepared from commercially available aromatic amines following published methods.²⁵ The salts can be stored for several weeks at $-20\text{ }^{\circ}\text{C}$. Potassium organotrifluoroborates **9a–c** were prepared as previously described.²⁶ ^1H and ^{13}C NMR spectra were recorded on a 500 or 200 MHz NMR spectrometer, and complete resonance assignments were performed from 2D COSY, HSQC, and HMBC spectra. ^1H and ^{13}C chemical shifts (δ) were referenced to internal solvent resonances and reported relative to SiMe_4 .

(*E,E,E*)-1,16-Bis(*tert*-butyloxycarbonyl)-1,6,11,16-tetrakis[(4-methylphenyl)sulfonyl]-1,6,11,16-tetraazahexadeca-3,8,13-trienepalladium(0) (3**).** In a 50 mL flask, (*E,E,E*)-1,16-bis(*tert*-butyloxycarbonyl)-1,6,11,16-tetrakis[(4-methylphenyl)sulfonyl]-1,6,11,16-tetraazahexadeca-3,8,13-triene¹⁷ (0.50 g, 0.48 mmol) was added to a solution of $\text{Pd}_2(\text{dba})_3$ (0.30 g, 0.53 mmol of Pd) in anhydrous and degassed acetonitrile (25 mL) under a nitrogen atmosphere. The reaction was stirred at room temperature for 5 h (TLC monitoring). The crude reaction mixture was filtered through Celite, and the solvent was evaporated under vacuum. The residue was purified by column chromatography on silica gel using mixtures of hexane/dichloromethane (1:10) as eluent to afford Pd(0) complex **3** (0.55 g, 65%) as a yellowish solid; mp $163\text{--}165\text{ }^{\circ}\text{C}$ (dec); IR (ATR) 2982, 1725, 1336, 1147, 1112, 1085 cm^{-1} ; ^1H NMR (500 MHz, CDCl_3) δ 1.41 (s, 18H), 1.58 (t, $J = 12\text{ Hz}$, 2H), 1.66 (br abs, 2H), 2.40 (s, 6H), 2.44 (s, 6H), 3.79 (t, $J = 12\text{ Hz}$, 2H), 4.00

(br abs, 4H), 4.41 (br abs, 2H), 4.66 (d, $J = 13.5\text{ Hz}$, 4H), 4.94 (d, $J = 13\text{ Hz}$, 2H), 7.31 (br abs, 8H), 7.63 (BB' part of a AA'BB' system, $J = 7\text{ Hz}$, 4H), 7.92 (BB' part of a AA'BB' system, $J = 7\text{ Hz}$, 4H); ^{13}C NMR (50 MHz, CDCl_3) δ 21.9, 22.0, 28.4, 48.7, 49.1, 49.4, 76.5, 80.0, 83.7, 85.0, 127.7, 128.5, 129.7, 130.3, 134.6, 137.8, 144.0, 144.6, 151.6; ESI-MS (m/z) 1169 $[\text{M} + \text{Na}]^+$. Anal. Calcd for $\text{C}_{50}\text{H}_{64}\text{N}_4\text{O}_{12}\text{PdS}_4$ (1147.75): C, 52.32; H, 5.62; N, 4.88; S, 11.18. Found: C, 52.38 and 52.09; H, 6.06 and 5.89; N, 5.06 and 5.09; S, 11.05 and 10.98.

(*E,E,E*)-1,6,11,16-Tetrakis[(4-methylphenyl)sulfonyl]-1,6,11,16-tetraazahexadeca-3,8,13-trienepalladium(0) (4**).** In a 50 mL flask, (*E,E,E*)-1,6,11,16-tetrakis[(4-methylphenyl)sulfonyl]-1,6,11,16-tetraazahexadeca-3,8,13-triene¹⁷ (0.15 g, 0.18 mmol) was added to a solution of $\text{Pd}_2(\text{dba})_3$ (0.12 g, 0.21 mmol of Pd) in anhydrous and degassed acetonitrile (10 mL) under a nitrogen atmosphere. The reaction was stirred at room temperature for 1.5 h (TLC monitoring). The solvent was evaporated under vacuum, and the residue was purified by column chromatography on silica gel using mixtures of ethyl acetate/dichloromethane of increasing polarity (0:1 to 1:20) to afford Pd(0) complex **4** (0.13 g, 75%) as a yellowish solid; mp $138\text{--}140\text{ }^{\circ}\text{C}$; IR (ATR) 3280, 3251, 1324, 1158 cm^{-1} ; ^1H NMR (500 MHz, CDCl_3) δ 1.45 (t, $J = 12\text{ Hz}$, 2H), 1.59 (br abs, 2H), 2.39 (s, 6H), 2.44 (s, 6H), 2.85 (br abs, 2H), 3.50–3.53 (m, 2H), 3.90–4.00 (m, 6H), 4.34 (d, $J = 13.5\text{ Hz}$, 2H), 4.54 (d, $J = 14\text{ Hz}$, 2H), 5.31 (br abs, 2H), 7.28 (br s, 4H), 7.34 (AA' part of a AA'BB' system, $J = 7\text{ Hz}$, 4H), 7.57 (BB' part of a AA'BB' system, $J = 7\text{ Hz}$, 4H), 7.79 (BB' part of a AA'BB' system, $J = 7.5\text{ Hz}$, 4H); ^{13}C NMR (50 MHz, CDCl_3) δ 21.9, 22.0, 46.2, 48.5, 48.6, 76.0, 80.3, 83.1, 127.4, 127.6, 130.3, 130.4, 134.7, 137.8, 144.0, 144.1; ESI-MS (m/z) 969 $[\text{M} + \text{Na}]^+$. Anal. Calcd for $\text{C}_{40}\text{H}_{48}\text{N}_4\text{O}_8\text{PdS}_4 \cdot \text{CH}_2\text{Cl}_2$ (1032.52): C, 47.69; H, 4.88; N, 5.43; S, 12.42. Found: C, 47.96 and 48.02; H, 5.15 and 5.16; N, 5.53 and 5.54; S, 12.23 and 12.23.

Crystal Structure Determination. Colorless crystals of **3** were obtained by slow diffusion of hexane into a dichloromethane/ethyl acetate solution and used for room temperature (300(2) K) X-ray structure determination. The measurement was carried out on a BRUKER SMART APEX CCD diffractometer using graphite-monochromated $\text{Mo K}\alpha$ radiation ($\lambda = 0.71073\text{ \AA}$) from an X-ray tube. The measurements were made in the range $2.03\text{--}28.41^{\circ}$ for θ . Full-sphere data collection was carried out with ω and φ scans. A total of 41 587 reflections were collected, of which 7226 [$R(\text{int}) = 0.0812$] were unique. Programs used: data collection, Smart version 5.631 (Bruker AXS 1997–02); data reduction, Saint+ version 6.36A (Bruker AXS 2001); absorption correction, SADABS version 2.10 (Bruker AXS 2001). Structure solution and refinement was done using SHELXTL version 6.14 (Bruker AXS 2000–2003). The structure was solved by direct methods and refined by full-matrix least-squares methods on F^2 . The non-hydrogen atoms were refined anisotropically. The H atoms were placed in geometrically optimized positions and forced to ride on the atom to which they are attached. The SQUEEZE routine of the program PLATON (Spek, A. L. PLATON, A Multipurpose Crystallographic Tool; Utrecht University, Utrecht, The Netherlands, 2005) was used to remove density peaks that could not be attributed to any chemical species.

Differential Scanning Calorimetry. The DSC experiments were performed using a Mettler Toledo DSC822e under inert conditions (continuous flow of 40 mL/min of high-purity N_2 , impurities less than 5 ppm). Sample masses were between 3 and 10 mg, and aluminum crucibles were used.

Biphenyl 10a: General Procedure for the Suzuki–Miyaura Reaction. A solution of benzenediazonium tetrafluoroborate **8a** (0.066 g, 0.34 mmol), potassium phenyltrifluoroborate **9a** (0.076 g, 0.41 mmol), and palladium(0) catalyst **1a** (0.015 g, 0.017 mmol) in 1,4-dioxane (8 mL) was stirred at room temperature until N_2 gas evolution ceased (15 h). Dichloromethane (10 mL) was added

(25) Roe, A. *Org. React.* **1949**, *5*, 193–228.

(26) For recent reviews, see: (a) Darses, S.; Genêt, J. P. *Eur. J. Org. Chem.* **2003**, 4313–4327. (b) Molander, G. A.; Figueroa, R. *Aldrichim. Acta* **2005**, *38*, 49–56. (c) Vedejs, E.; Chapman, R. W.; Fields, S. C.; Lin, S.; Schrimpf, M. R. *J. Org. Chem.* **1995**, *60*, 3020–3027.

to the reaction mixture, the organic layer was washed with saturated NaCl aqueous solution (15 mL) and H₂O (2 × 15 mL) and dried with anhydrous sodium sulfate, and the solvents were evaporated. The residue was purified by column chromatography on silica gel (hexanes/ethyl acetate, 9:1) to give biphenyl **10a** (0.034 g, 63% yield), and when the polarity was increased (hexanes/ethyl acetate, 7:3) **1a** was recovered quantitatively (0.015 g, 100% recovery).

Acknowledgment. Financial support from the Spanish Ministry of Education and Science (MEC, Project Nos. CTQ2005-04968, CTQ2005-08797, CTQ2006-01080, MAT2006-11144) and the Generalitat de Catalunya (Project Nos. 2005SGR00305, 2005SGR00666) is gratefully acknowledged. A.D. and J.M. thank Spanish Ministry of Education

and Science for a predoctoral grant. We also thank Prof. Pere Roura for helpful suggestions and Xavier Fontrodona from Research Technical Services of the UdG for X-ray diffraction data.

Supporting Information Available: NMR spectra of complexes **3** and **4** and DSC curves for all compounds. CIF file containing X-ray crystallographic data for **3**. This material is available free of charge via the Internet at <http://pubs.acs.org>. The supplementary crystallographic data for this paper (CCDC 690372) can also be obtained free of charge via <http://www.ccdc.cam.ac.uk/deposit>.

OM800544H